Symmetrical dispersion compensation for standard monomode-fiber-based communication systems with large amplifier spacing

D. Breuer

Technische Universität Berlin, Fachbereich 12, Fachgebiet Hochfrequenztechnik, Einsteinufer 25, 10587 Berlin, Germany

F. Küppers and A. Mattheus

Deutsche Telekom AG, Technologiezentrum, Postfach 100003, D-64276 Darmstadt, Germany

E. G. Shapiro

Institute of Automatics and Electrometry, 630090 Novosibirsk, Russia

I. Gabitov and S. K. Turitsyn

Institut für Theoretische Physik I, Heinrich-Heine-Universität Düsseldorf, 40225 Düsseldorf, Germany

Received February 19, 1997

Optical 10-Gbit/s return-to-zero pulse transmission in cascaded communication systems using dispersion compensation of the standard monomode fiber with large amplifier spacing is examined. It is shown that pulse distortions that are due to Kerr nonlinearity are significantly diminished by symmetrical ordering of the compensation sections when the total number of precompensation and postcompensation sections is equal. Repositioning of these sections is not critical. © 1997 Optical Society of America

Large amplifier spacing, of the order of 100 km, is desirable for the design of optical communication networks because it reduces the number of repeater stations needed and thus the total cost of the link. Evidently, with increasing amplifier spacing, higher input powers are required for a good signal-to-noise ratio. The effects of nonlinearity, therefore, increase in such a system. There are various ways to diminish the impact of nonlinearity on the transmission. In conventional transmission systems using a nonreturn-to-zero format the dispersion compensation, based on the eponymous dispersion-compensation fiber (DCF), has been successfully applied to suppress four-photon mixing (see, e.g., Ref. 1 and references therein). In soliton-based transmission systems the nonlinearity is balanced by dispersion. For stable soliton transmission, however, specific requirements have to be fulfilled: a minimum averaged optical power is required for balancing dispersion and the amplifier spacing has to be smaller than the dispersion length. Therefore traditional soliton transmission at 10 Gbits/s over an already installed standard fiber network operating at 1.55 μm necessitates unrealistically small amplifier spacings. Long-haul optical communication systems with relatively large amplifier spacing in excess of 100 km that use low-dispersion fibers have already been realized for both nonreturn-to-zero signal[1] and soliton[2,3] transmission. Cascaded communication systems with large amplification periods that use standard telecommunication fiber with high local dispersion [$\approx$17 ps/(nm $\times$ km) at 1.55 μm] have been comparatively less studied, although this problem is directly associated with upgrading of existing fiber networks.

By means of numerical simulations and using the variational approach, we study various schemes for dispersion management for links with large amplifier spacing with the goal of minimizing the influence of nonlinearity for a cascaded system. Single-channel soliton transmission over 960 km of standard monomode fiber (SMF) lines with periodically placed erbium-doped fiber amplifiers (EDFA's) (the SMF spacing is 120 km) operating at 1.55 μm and periodic compensation by additional fibers with negative dispersion coefficients have been considered.

The evolution of the complex field envelope along the line is governed by the nonlinear Schrödinger equation

$$i\frac{\partial A}{\partial z} - \frac{1}{2}\beta_2^{(1,2)}\frac{\partial^2 A}{\partial t^2} + \sigma^{(1,2)}|A|^2 A = i\left[-\gamma^{(1,2)} + \sum_{k=1}^{N} r_k^{1,2}\delta(z - z_k^{(1,2)})\right] = iG^{(1,2)}(z)A, \quad (1)$$

where superscripts 1 and 2 correspond to SMF and DCF, respectively, t is the retarded time, $|A|^2 = P$ is the optical power in watts, $\beta_2^{(1,2)}$ is the first-order group-velocity dispersion, $\sigma^{(1,2)} = (2\pi n_2)/(\lambda_0 A_{\text{eff}}^{(1,2)})$ is the nonlinear coefficient, n_2 is the nonlinear refractive index, $\lambda_0 = 1.55$ μm is the carrier wavelength, $A_{\text{eff}}^{(1,2)}$ is the effective fiber area, $z_k (k = 1, \ldots, N)$ are the amplifier locations, and the amplification distances are $z_a^{(1)} =$ 120 km (SMF) and $z_a^{(1)} = 24$ km (DCF). Amplification coefficients are $r^{1,2} = [\exp(\gamma^{1,2} z_a^{1,2}) - 1]$, respectively, for SMF and DCF pieces. The loss coefficient $\gamma^{(1,2)} = 0.05 \ln(10)\alpha^{(1,2)}$ [km^{-1}] accounts for the fiber attenuation along an amplifier span; here $\alpha^{(1,2)}$ is given in decibels per kilometer.

As shown in Refs. 4–6, an approximate analytical description of the evolution of the input pulse having the form $|A(t)|^2 = P_0/\cosh^2(t/t_0)$ along the transmis-

0146-9592/97/130982-03$10.00/0

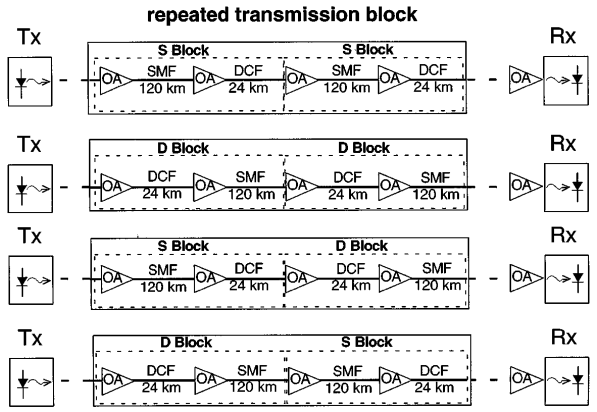

Fig. 1. Block schematics of the communication system design. Tx, transmitter; Rx, receiver; OA, optical amplifier.

sion system with attenuation and dispersion compensation is given by

$$A(z,t) = |A|\exp(i\phi), \qquad |A(z,t)|^2 = \frac{t_0}{b(z)}\,\frac{P_0}{\cosh^2[t/b(z)]},$$
$$\frac{\partial\phi}{\partial t} = 2\,\frac{\nu(z)t}{b(z)}, \tag{2}$$

where $b(z)$ and $\nu(z)$ are found from

$$b_z = -2\beta_2^{(1,2)}\nu,$$
$$\nu_z = -\frac{2}{\pi^2}\left\{\frac{\beta_2^{(1,2)}}{b^3} + \frac{P_0\sigma^{(1,2)}\exp[2\int^z G^{(1,2)}(z')\mathrm{d}z']}{b^2}\right\}, \tag{3}$$

with initial conditions $b(0) = t_0$ and $\nu(0) = 0$, where P_0 is the input pulse power and t_0 is the characteristic pulse width.

The various system setups are depicted in Fig. 1. Dispersion management is performed by DCF units. The transmission line consists of equal numbers of pieces of 120-km SMF and 24-km DCF. The total link is constructed from 16 amplifier spans. The amplifier gain equalizes the loss between consecutive amplifiers for both SMF and DCF pieces. As shown in Fig. 1, two basic elements were used for transmission line construction, representing two schemes, postcompensation and precompensation. D denotes a precompensation section when a 24-km DCF is followed by an EDFA, then 120-km SMF, and finally an EDFA. S denotes the postcompensation sequence: 120-km SMF, EDFA, 24-km DCF, and EDFA. We define symmetrical compensation as schemes in which the total number of D and S sections is equal. We used the following parameters in our simulations: The transmitter emits hyperbolic-secant-shaped pulses with T_{FWHM} of 25 ps and a high peak power of 13.7 mW to maintain a good signal-to-noise ratio. The nonlinear refractive index was $n_2 = 3 \times 10^{-20}$ m^2/W. Attenuation was $\alpha^{(1)} = 0.22$ dB/km in the SMF and $\alpha^{(2)} = 0.8$ dB/km in the DCF. The effective fiber area $A_{\mathrm{eff}}^{(1)}$ was 95 μm^2 for SMF and 30 μm^2 for DCF. The dispersion coefficients were $D^{(1)} = 16.2$ ps/(nm $\times$ km) for SMF and $D^{(2)} = -81.0$ ps/(nm $\times$ km) for DCF.

The pulse dynamics in the transmission systems under consideration is determined by the combined action of self-phase modulation and varying chromatic dispersion. It should be pointed out that these effects are not additive and depend critically on the order in which dispersion compensation is realized. Strong interference of self-phase modulation and varying chromatic dispersion actions leads to a rich variety of possible configurations for dispersion management. Let us demonstrate advantages of using what we call symmetrical compensation. The results of simulations are presented in Figs. 2–4. Figure 2 plots peak power evolution at the amplifiers (at the end of the compensation sections) along the line for the precompensation, postcompensation, and symmetrical compensation schemes. After passing the postcompensating line the optical pulse broadens; the precompensation scheme leads to effective pulse compression. Therefore it is natural to assume that by alternating cells with postcompensation and precompensation one can balance these two opposite tendencies. One can see the advantage of using symmetrical compensation. Figure 3 presents pulse-width evolution for the same configurations as in Fig. 2. As Figs. 2 and 3 show, within the symmetrical schemes the performance does not depend critically on the positioning order of D and S sections. One can also see from these figures that results derived by the variational approach are in a rather good agreement with results obtained by direct numerical simulations. Some deviation of the numerical results from the

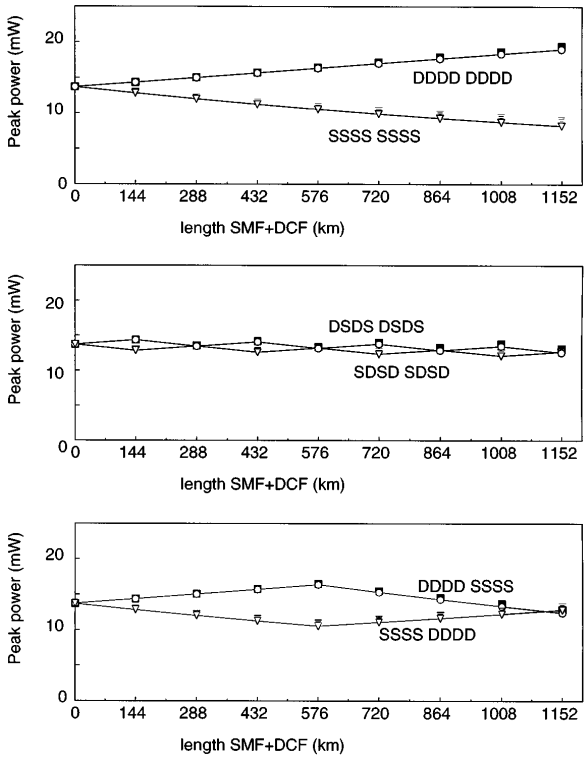

Fig. 2. Peak power evolution (shown at the ends of the sections) over 16 amplifications for different configurations, including precompensation (DDDD DDDD) and postcompensation (SSSS SSSS), and various versions of the symmetrical compensation. Open circles indicate upper curves and open triangles indicate lower lines for direct numerical simulations; filled squares and hatched triangles indicate the variational approach.

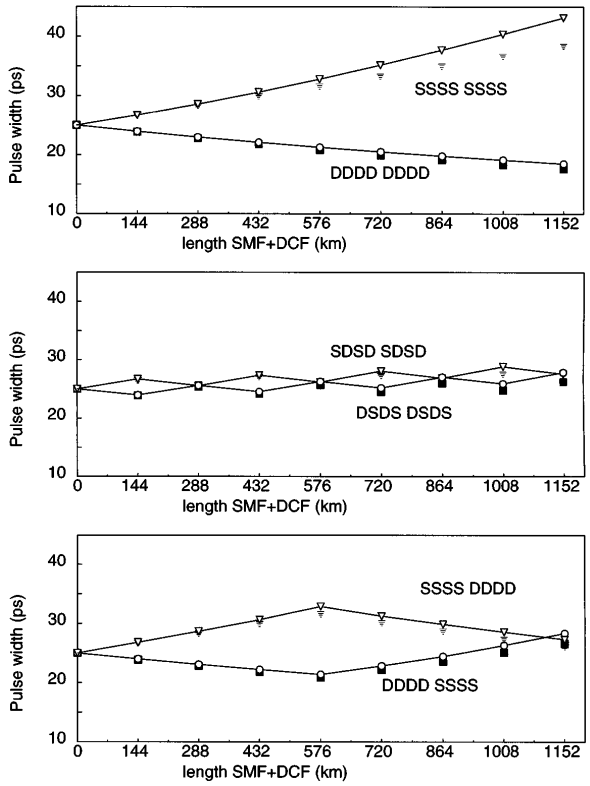

Fig. 3. Same as in Fig. 2 but for the pulse-width evolution. Open triangles indicate upper curves and open circles indicate lower lines for direct numerical simulations; hatched triangles above and filled squares below indicate the variational approach.

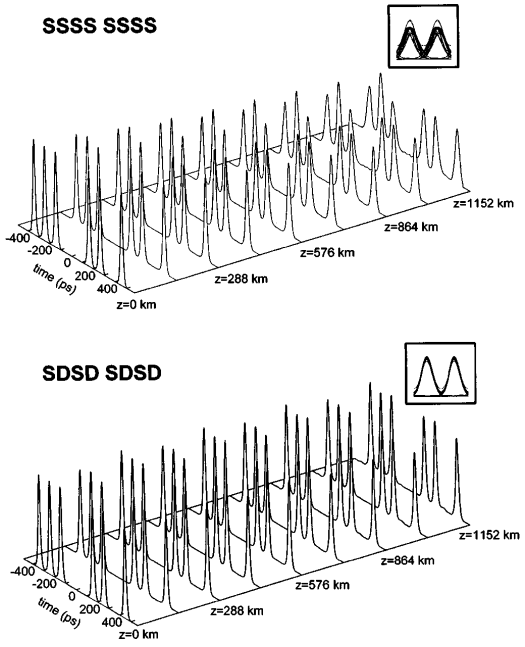

Fig. 4. Improvement of transmission in the case of symmetrical compensation. Pattern propagation and eye diagrams for postcompensation (SSSS SSSS) and for symmetrical compensation (SDSD SDSD).

curves obtained by the variational method is due to radiation that is emitted by the central pulse, because the approximate variational approach well describes only the dynamics of the main peak.

To show the potential of the new symmetrical compensation schemes, we also investigated pattern propagation. Figure 4 shows the pattern dynamics and eye diagrams for postcompensation (SSSS SSSS) and for symmetrical compensation (SDSD SDSD). As is obvious from Fig. 4, the system performance in terms of eye opening and temporal and amplitude jitter is significantly improved for the symmetrical configurations. In the symmetrical scheme the initial pattern is restored at the end of the link. For the postcompensation scheme, however, the signal is severely distorted by nonlinearities. It is clear from the eye diagrams in Fig. 4 that the amplitude fluctuations are considerably reduced by the symmetrical compensation scheme. The eye-closure penalty is reduced from 2.48 dB (postcompensation scheme) to 0.71 dB for symmetrical compensation.

We have studied different schemes of dispersion compensation managements in cascaded transmission systems based on the standard monomode fibers with large amplifier spacing of 120 km. The system performance is substantially improved by use of an equal number of precompensation and postcompensation sections in the compensation scheme. This result does not depend critically on the order of section repositioning if the number of precompensating sections is equal to the total number of postcompensating sections in the chain. The suggested design permits quasi-stable pulse transmission over 960-km SMF with 120-km amplifier spacing (when the input pulse is approximately restored after such distance) even without a mandatory requirement for anomalous path-average dispersion (cf. Refs. 4, 6, and 7). Numerical results are in good agreement with results of the semianalytical variational approach.[4–6]

E. G. Shapiro acknowledges the support of the Russian Foundation for Basic Research (grant 96-02-19131-a) and Volkswagen-Stiftung (grant I/71 824).

References

1. N. S. Bergano, C. D. Davidson, D. L. Wilson, F. W. Kerfoot, M. D. Tremblay, M. D. Levanas, J. P. Morreale, J. D. Erankow, P. C. Corbett, M. A. Mills, G. A. Ferguson, A. M. Vengsarkar, J. R. Pedrazzani, J. A. Nagel, J. L. Zyskin, and J. W. Sulhoff, in *Optical Fiber Communication Conference*, Vol. 2 of 1996 OSA Technical Digest Series (Optical Society of America, Washington, D.C., 1996), postdeadline paper PD23-1.
2. L. F. Mollenauer, P. V. Mamyshev, and M. J. Neubelt, Electron. Lett. **32,** 471 (1996).
3. M. Nakazawa and H. Kubota, Electron. Lett. **31,** 216 (1995).
4. I. Gabitov and S. K. Turitsyn, Sov. JETP Lett. **63,** 861 (1996).
5. A. Berntson, D. Anderson, M. Lisak, M. L. Quairog-Teixeiro, and M. Karlsson, Opt. Commun. **130,** 153 (1996).
6. I. Gabitov, E. G. Shapiro, and S. Turitsyn, Opt. Commun. **134,** 317 (1996).
7. N. Smith, F. M. Knox, N. J. Doran, K. J. Blow, and I. Bennion, Electron. Lett. **32,** 55 (1995).